DRAFT VERSION DECEMBER 14, 2011
Preprint typeset using LaTeX style emulateapj v. 5/2/11

A GENERAL RELATIVISTIC EXTERNAL COMPTON-SCATTERING MODEL FOR TEV EMISSION FROM M87

YU-DONG CUI[1], YE-FEI YUAN[1a], YAN-RONG LI[2], JIAN-MIN WANG[2]
1 Key Laboratory for Research in Galaxies and Cosmology, Department of Astronomy, University of Sciences and Technology of China, CAS, Hefei, Anhui 230026, China
2 Key Laboratory for Particle Astrophysics, Institute of High Energy Physics, CAS, 19B Yuquan Road, Beijing 100049, China
Draft version December 14, 2011

ABSTRACT

M87 is the first detected non-blazar extragalactic Tera-Electron-Volt (TeV) source with rapid variation and very flat spectrum in the TeV band. To explain the two-peaks in the spectral energy distribution (SED) of the nucleus of M87 which is similar to those of blazars, the most commonly adopted models are the synchrotron self-Compton scattering (SSC) models and the external inverse Compton scattering (EIC) models. Considering that there is no correlated variation in the soft band (from radio to X-ray) matching the TeV variation, and the TeV sources should not suffer from the $\gamma\gamma$ absorption due to the flat TeV spectrum, the EIC models are advantageous in modeling the TeV emission from M87. In this paper, we propose a self-consistent EIC model to explain the flat TeV spectrum of M87 within the framework of fully general relativity, where the background soft photons are from the advection-dominated accretion flow (ADAF) around the central black hole, and the high energy electrons are from the mini-jets which are powered by the magnetic reconnection in the main jet (Giannios et al. 2010). In our model, both the TeV flares observed in the years of 2005 and 2008 could be well explained: the $\gamma\gamma$ absorption for TeV photons is very low, even inside the region very close to the black hole $20R_g \sim 50R_g$; at the same region, the average EIC cooling time ($\sim 10^2 \sim 10^3 s$) is short, which is consistent with the observed time scale of TeV variation. Furthermore, we also discuss the possibility that the accompanying X-ray flare in 2008 is due to the direct synchrotron radiation of the mini-jets.

Subject headings: black hole physics — galaxies: individual (M87)

1. INTRODUCTION

Unlike blazars and the Galactic sources (e.g. SNRs), which composite the most population of TeV sources, M87 is the first discovered radio galaxy with TeV radiation. Recently three other radio galaxies Centaurus A, 3C66B and IC310 were also identified as TeV sources (Aharonian et al. 2009; Aliu et al. 2009; Aleksić et al. 2010). Comparing to blazars, M87 has much milder variations in both optical and X-ray band; most importantly, the prominent kpc-scale jet of M87 has a very large viewing angle $\sim 30^\circ$ with respect to the line of sight (Bicknell & Begelman 1996; Aharonian et al. 2006). In 2005, rapid TeV variation ($1-2$days) was discovered with flat spectrum for the first time, but without correlated X-ray variation from the nuclear core (Aharonian et al. 2006). While in 2008, the radio, X-ray, TeV joint observation discovered that TeV flares lasts 2 weeks accompanied with an X-ray flare and a radio flare inside the unresolved nuclear core ($30 \times 60R_s$) as well as with a radio blob moving out of the unresolved core (Acciari et al. 2009). Here R_s used in the VLBA observations are based on the black hole (BH) mass of M87 $M_{BH} = 6 \times 10^9 M_\odot$ (Gebhardt & Thomas 2009). Recently, a TeV flare in 2010 which is very similar to the previous TeV flares in 2005 and 2008 was reported. Further observations at X-rays and radio find the correlated X-ray flare, but no enhanced radio flux from the core (Abramowski et al. 2011; Harris et al. 2011). In this paper, we adopt $M_{BH} = 3 \times 10^9 M_\odot$ (Macchetto et al. 1997) to be consistent with the advection-dominated accretion flow (ADAF) models and the mini-jet models in the previous studies (Li et al. 2009; Giannios et al. 2010).

Although M87 has a large viewing angle, it is very near to the Earth with a distance of ~ 16.7Mpc. Owing to its proximity, it is proposed that M87 might be a misaligned blazar (Tsvetanov et al. 1998). Whereas blazars are believed to have jets beaming towards us, TeV sources in M87 could be shocks with relativistic bulk velocity inside the jets. Recent observed minute-scale variation from galaxies like Mrk 421 (Fossati et al. 2008) and PKS 2155-304 (Aharonian et al. 2007) indicates that TeV sources should be compact and very close to the BH. Comparing to the TeV flares of blazars, the slower variation ($1-2$ day) detected in M87 could be the results of too few observed TeV photons (each data point requires integration of photons for the whole night) or the much lower Doppler factor of the bulk velocity of the TeV sources due to the large inclination. Furthermore, unlike the steeper TeV spectrum of blazars, the much flatter TeV spectrum of M87 could be mainly due to the lack of $\gamma\gamma$ absorption. The large viewing angle may play an important role in avoiding $\gamma\gamma$ absorption within the jet; thanks to its proximity and the dimness of its host galaxy, the absorption to TeV photon from M87 caused by the galactic and the intergalactic background soft photons, as well as the cosmic background photons is rather weak (Neronov & Aharonian 2007).

To explain the spectral energy distribution (SED) of the nucleus of M87, the one zone synchrotron self-Compton(SSC) models, which have been applied to the TeV flares in blazars (e.g. Tavecchio et al. 1998; Katarzyński et al. 2001), face difficulties in fitting the two peaks in the SED, however, in the multi-zone SSC models, the TeV source is separated from the soft ones, therefore the whole SED could be easily fitted as long as there are enough SSC blobs with specific locations, electron distributions and bulk velocity (e.g. Tavecchio & Ghisellini 2008; Lenain 2007; Georganopoulos et al. 2005). The multi-zone SSC models could also provide better explanation for the rapid variation, and the orphan TeV flares (the variations in the soft band can not connect with

[a] corresponding author: yfyuan@ustc.edu.cn

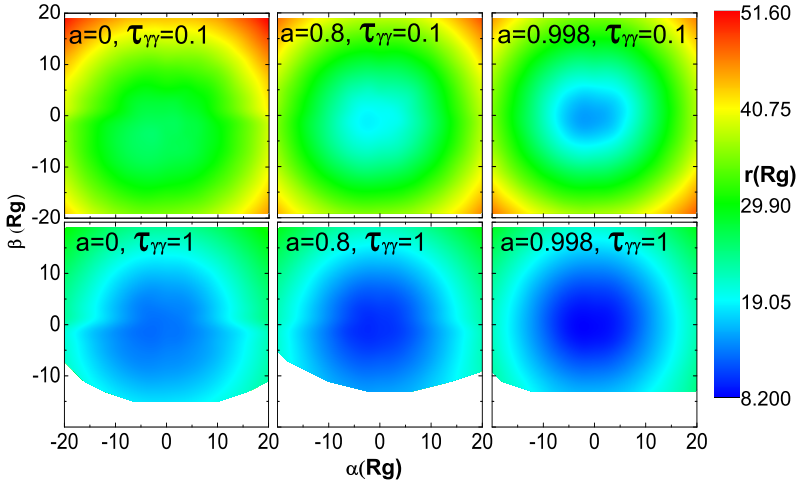

FIG. 1.— The contour of $\tau_{\gamma\gamma}$ = 0.1 or 1 in the α, β plane. Where r represents the distance to the BH in the Boyer-Lindquist frame. The viewing angle is taken to be 30°. The blank region in the lower panels is the region with $\tau_{\gamma\gamma} \leq 1$.

the TeV variation). Furthermore, considering the very flat power-law SED of M87 in the TeV band with index $p \simeq -2.2 \sim -2.6$, the $\gamma\gamma$ absorption provides crucial constrains on the SSC models. So far, most of the SSC models still have problems in explaining the very flat TeV spectrum due to the certain $\gamma\gamma$ absorption, therefore the external inverse Compton (EIC) process could be more likely responsible for the TeV flare (Begelman et al. 2008; Giannios et al. 2009, 2010). In the EIC models, the TeV source is far away from the soft one, or has the relativistic bulk velocity with respect to the soft one, thus the $\gamma\gamma$ absorption can be reduced.

In those models mentioned above, how the very high energy (VHE) particles are produced is still an open question. It is generally believed that VHE particles are accelerated by the shocks in jets. There are some other possibilities include the mini-jets powered via the magnetic reconnection in the main jet (Giannios et al. 2010, and references therein); the magnetic centrifugal acceleration in the vicinity of BH (Neronov & Aharonian 2007; Rieger & Agaronian 2008), and so on. In the mini-jets model (Giannios et al. 2010), magnetic reconnection within the main jet produces two oppositely directed (in the rest frame of the main jet) mini-jets, in the laboratory frame, one of them always points within the angle of the main jet and is observable in blazars because their jets point at us. The other mini-jet (its counterpart) points outside the opening angle of the main jet and is potentially observable to off-axis observers in case of the misaligned jets, such as those of M87 and Centaurus A. In a word, the great advantage of the mini-jets model is that even at large inclination, mini-jets with a high bulk speed can still be detected, which is helpful for explanation of the fast TeV variation from M87. After all, in order to avoid the $\gamma\gamma$ absorption, the energy density of the soft synchrotron photons in the TeV source must be limited, therefore, the minimal Lorentz factor of the VHE particles is generally assumed to be 10^{3-4} and the strength of the magnetic field in the TeV source below several Gauss (Giannios et al. 2010). Beside the direct inverse Compton process of the VHE electrons, there are also some alternative models to produce the SED of the TeV flares, such as the hadronic models including, among which, the interaction between the VHE protons and soft photons (Reimer et al. 2004) and the proton-proton collision process when a red giant was passing the base of the jet (Barkov et al. 2010).

In this paper, we develop a fully general relativity EIC model for explaining the TeV emission from M87, in which the soft photons emanate from the ADAF around the BH. In §2, we investigate the safe zone of TeV photons (the $\gamma\gamma$ optical depth is below unity). The technical details of our fully general relativity EIC model can be found in §3. The numerical results and the discussions are given in §4 and §5, respectively.

2. CONSTRAINTS ON THE LOCATION OF TEV SOURCES

The rapid TeV variation of M87 ($t_{\rm var} < 1-2$ days) found both in 2005, 2008 and 2010 indicates that the TeV photons should come from a compact source very close to the black hole ($R_{\rm TeV} \lesssim ct_{\rm var}\delta_{\rm D}$, where $\delta_{\rm D}$ is the Doppler factor of the source). Especially the TeV flare in 2008, which is accompanied with a radio flare, lies inside the unresolved region and there is a radio blob moving outwards. Again, this indicates that the TeV source might be near to the BH and its distance might be less than $\sim 100R_{\rm s}$ (Beilicke et al. 2010).

As mentioned above, beside the constrains from the VLBA radio image and the variation time scale of the TeV emission, the background soft photons could also lay strong constrains on the location of the TeV sources, in consideration of the $\gamma\gamma$ absorption. Both the TeV flares in 2005, 2008 and 2010 had shown very flat power-law spectrum ($0.1 \sim 10$ TeV) strongly suggesting quite weak $\gamma\gamma$ absorption. Therefore, the EIC process seems to be a more plausible mechanism to produce the flat TeV spectrum, while the SSC models suffer from certain $\gamma\gamma$ absorption (Giannios et al. 2010). Even in the EIC models, if the source of soft photons is from a homogeneously isotropic blob whose size is about $50R_{\rm g}$ and infrared luminosity is about $L_{\rm IR} \sim 10^{41}$erg/s, the location of the TeV sources could be still limited to be no deeper than $\sim 5R_{\rm g}$ inside that blob.

The observed soft photons from M87 could be mainly either from the disk or from the outflow/jet. According to the VLBI observations of M87, its jet is well known with a large inclination. However, the base of the jet seems to have a large opening angle ($\theta_{\rm open} \sim 30^\circ$ inside the region $\sim 70R_{\rm s}$, Junor et al. 1999; Ly et al. 2007; Acciari et al. 2009), therefore the jet might contribute to the observed soft emission. Due to the slight variation of the observed flux of soft photons (from radio to X-ray) from M87 nucleus, here we suggest that the observed soft photons are mainly from the accretion disk around the central black hole as in Li et al. (2009).

By applying the ADAF model to the nuclear emission of M87, Li et al. (2009) obtained the accretion rate of ADAF in M87, generally consistent with the previous estimate of the Bondi accretion rate from the Chandra X-ray observation (Di Matteo et al. 2003). They then calculated optical depth of the radiation fields from the ADAF to TeV photons due to $\gamma\gamma$ absorption. The resultant optical depth suggests that the location of TeV sources should be larger than $\sim 10R_{\rm g}$, in order to avoid the significant $\gamma\gamma$ absorption to a 10 TeV photon (Wang et al. 2008; Li et al. 2009). Here we try to map a more detailed safe zone ($\tau_{\gamma\gamma} \leq 1$) for TeV photons in the vicinity of BH. As in Li et al. (2009). For this purpose, we calculate the optical depth ($\tau_{\gamma\gamma}$) to 10 TeV photons emanating from vicinity of the central BH in the Kerr spacetime. The TeV photons move outwards along their geodesic trajectories and reach the observer's sky at points described by the impact parameters α and β. Here α and β respectively represent the displacement of the image perpendicular to the projection of the rotation of the black hole on the sky and the displacement parallel to the projection of the axis (see e.g. Fig. 1 of Li et al. 2009). The resultant contour of $\tau_{\gamma\gamma}$ as a function of the location of the TeV sources for $\tau_{\gamma\gamma}$ = 1 and 0.1 in the $\alpha\beta$ plane can be obtained (see Fig. 1).

As shown in Fig. 1, it is obvious that the larger the spin a, the deeper the safe zone. For instance, for $a = 0.998$, the safe zone can reach even to $10R_{\rm g}$ along some trajectories of 10TeV photons, the reason is that for larger BH spin, the infrared-UV radiation is concentrated in the inner disk. Therefore, the colliding angle between the soft photons and the TeV photons in the mini-jets is smaller, significantly reducing the $\gamma\gamma$ absorption. Besides, in the panels of $a = 0, 0.8$, the asymmetricity is caused by the rotation of the disk and the viewing angle(30°) of the observer. While in the panels of $a = 0.998$, since the disk become a more compact source of soft photons, the asymmetricity caused by the disk become weaker.

3. FULLY GENERAL RELATIVITY EXTERNAL-INVERSE COMPTON MODEL

3.1. *The TeV source*

In our EIC model, following Giannios et al. (2010), the mini-jets powered by magnetic energy in the jet correspond to be the TeV sources. For a clarity, we present the details of the model in what follows.

The strength of the magnetic field in the main jet is estimated as,

$$\frac{B_j^2}{4\pi} = \left(\frac{L_{j,iso}}{4\pi r_j^2 c\Gamma_j^2}\right)\left(\frac{\sigma}{1+\sigma}\right), \tag{1}$$

where B_j is the magnetic strength, $L_{\rm j,iso}$ ($\sim 10^{45}$ erg/s) is the observed isotropic power of the jet of M87 (Bicknell & Begelman 1996; Reynolds et al. 1996; Owen et al. 2000; Stawarz et al. 2006; Bromberg & Levinson 2009), $A_{\rm j}$ ($\pi {r_{\rm j}}^2$) is the cross sectional area of the jet, σ is the ratio of the magnetization energy to the kinetic energy of the main jet, Γ_j is the Lorentz factor of the main jet, and c is the light speed.

Although the inclination of the jet is about 30^0, the mini-jets (blobs of plasma with characteristic Lorentz factor $\Gamma_{\rm co}$ at angle $\theta_{\rm mini}$ with respect to the jet in the jet rest frame) are capable of beaming towards us with a high bulk velocity $\Gamma_{\rm em} = \Gamma_{\rm j}\Gamma_{\rm co}(1+\beta_{\rm j}\beta_{\rm co}\cos\theta_{\rm mini})$ in the laboratory frame. The bulk Lorentz factor of the mini-jets in the jet rest frame is about $\Gamma_{\rm co} \sim \sigma^{1/2}$, which corresponds to the Alfvén speed of the plasma in the jet. The characteristic thermal Lorenz factor of the electrons in the mini-jets rest frame is about $\gamma'_{\rm ch} \sim f\sigma^{1/2} m_{\rm p}/m_{\rm e}$. The energy distribution of the high energy electrons is assumed to be

$$N'_e(\gamma') = N_e(\gamma)/\delta_D^3 = N_0\gamma'^p, \tag{2}$$

where $10^4 \lesssim \gamma' = \gamma/\delta_D < \infty$, $p \lesssim -3.2$. In our canonical model, Γ_j is taken to be 5, and $\Gamma_{\rm em}$ = 12 ($\delta_{\rm D}$ = 23, if the mini-jets are beaming toward us). These parameters are consistent with the original mini-jets model of Giannios et al. (2010).

3.2. *The Local Soft Radiation Field*

In our EIC model, we assume that the soft photons are from the accretion disk and the TeV source (mini-jets) is located along the major axis of jet with a height $H_{\rm TeV}$ above the central black hole. To investigate the EIC process, we apply the same ray-tracing technique as discussed in Li et al. (2009). In Li et al. (2009), the authors discussed the optical depth of the TeV photons due to colliding with the soft photons from the accretion disk. In this work, we investigate the Compton scattering of the soft photons from the disk by the VHE electrons in the mini-jets (as shown in Fig. 2), therefore, we just simply replace the TeV photons in the model of Li et al. (2009) with the VHE electrons.

To obtain the flux density of the soft photons from the disk, the global dynamical structure of the ADAF, such as the four velocity of the fluid in the disk, the temperature of ions and electrons, should be determined first; then the local emergent spectra $I_{\nu_d}(r_{\rm d})$ at the radius $r_{\rm d}$ in the rest frame of the fluid can be calculated. Using the ray-tracing technique, the observed SED can be obtained to fit the multi-wavelength observations of M87. The fitting parameters of the ADAF are obtained by Li et al. (2009). In what follows, we summarize the procedure to obtain the radiation energy density of the soft photons from the direction $(\theta_{\rm s}, \phi_{\rm s})$ at the colliding location $(r_{\rm c}, \theta_{\rm c}, \phi_{\rm c})$.

In the locally non-rotating frame (LNRF), at the interacting place $(r_{\rm c}, \theta_{\rm c}, \phi_{\rm c})$, the two motion constants of the soft photons ($\lambda_{\rm s}$, $\mathcal{Q}_{\rm s}$) are related with their traveling direction $(\theta_{\rm s}, \phi_{\rm s})$ as follows:

$$\lambda_{\rm s} = \frac{\mathscr{A}}{1+\omega\mathscr{A}}, \quad \mathcal{Q}_{\rm s} = \mathscr{B}^2 - (a\cos\theta_{\rm c})^2 + (\lambda_{\rm s}\cot\theta_{\rm c})^2. \tag{3}$$

where,

$$\mathscr{A} = \frac{\sin\theta_s \sin\phi_{\rm s} \sin\theta_{\rm c} A}{\Sigma\Delta^{1/2}}, \quad \mathscr{B} = \frac{\sin\theta_s \cos\phi_{\rm s} A^{1/2}(1-\omega\lambda_{\rm s})}{\Delta^{1/2}}, \tag{4}$$

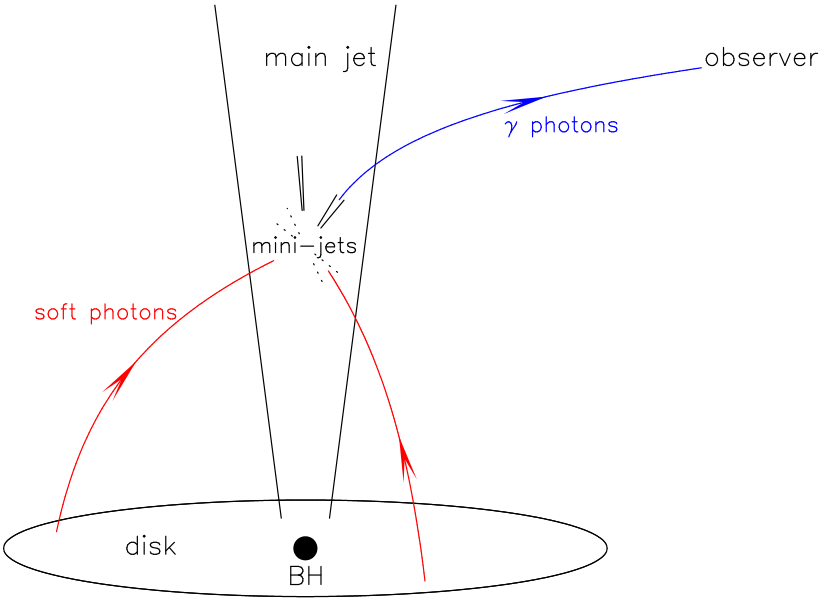

FIG. 2.— A schematic picture for the disk dominating external Compton-scattering model. A mini-jet is beaming toward the infinity observer, and the soft photons are from the disk.

where A, Σ, Δ, and ω are the metric functions defined in Bardeen et al. (1972).

After knowing the constants of motion $\lambda_{\rm s}$ and $\mathcal{Q}_{\rm s}$, the soft photons can be traced back to the disk at certain radius $r_{\rm d}$ by solving the geodesic equations (e.g. Bardeen et al. 1972; Yuan et al. 2009)

$$\mathscr{T} = \pm\int_{r_{\rm c}}^{r_{\rm d}} \frac{{\rm d}r}{\sqrt{\mathcal{R}(r)}} = \pm\int_{\theta_{\rm c}}^{\theta_{\rm d}} \frac{{\rm d}\theta}{\sqrt{\Theta(\theta)}} \tag{5}$$

where $\mathscr{T}$ is the affine parameter and the $\pm$ signs represent the increment (+) or decrement (–) of r and θ coordinates along the trajectory, respectively.

Along these trajectories, the redshift factor $g_{\rm s}$ for a soft photon travels from disk to the IC interaction location can be obtained by

$$g_s = \frac{\nu_s}{\nu_d} = \frac{e^{\mu}_{(t)}({\rm LNRF}){\rm P}^{\rm s}_{\mu}\Big|_{r_{\rm c}}}{e^{\mu}_{(t)}({\rm LRF}){\rm P}^{\rm s}_{\mu}\Big|_{r_{\rm d}}} = \frac{e^{-\nu}(1-\omega\lambda_{\rm s})|_{r_{\rm c}}}{\gamma_r\gamma_\phi e^{-\nu}\left[1-\Omega\lambda_{\rm s}\mp\dfrac{\beta_r\mathcal{R}(r)^{1/2}}{\gamma_\phi A^{1/2}}\right]\Big|_{r_{\rm d}}}. \tag{6}$$

where $\nu_{\rm s}$ and $\nu_{\rm d}$ are the frequency of the soft photon at the colliding place and the disk, and $\gamma_r = (1-\beta_r^2)^{-1/2}$ and $\gamma_\phi = (1-\beta_\phi^2)^{-1/2}$ are the Lorentz factors of the radial and azimuthal velocity of the fluid in the accretion disk, respectively.

According to the Liouvell theorem, the final radiation energy density of the soft photons at the IC location $(r_{\rm c}, \theta_{\rm c}, \phi_{\rm c})$ can be written as

$$U_{\rm s}(h\nu_{\rm s}, \theta_{\rm s}, \phi_{\rm s}, r_{\rm c}, \theta_{\rm c}, \phi_{\rm c}) = \frac{I_{\nu_{\rm d}}(h\nu_{\rm d}, r_{\rm d})g_{\rm s}^3}{c}, \tag{7}$$

where h is the Planck's constant.

3.3. *The VHE electrons*

After determining the radiation energy density of the soft photons $U_{\rm s}$ at the colliding points, the direction of motion of the VHE electrons which produce the observed TeV photons is needed to calculate the TeV spectra. Due to the effects of special relativity, it is a reasonable assumption that both the direction of the relativistic electrons and that of the TeV photons are the same. Denoting the two constants of the motion of the TeV photons as $\lambda_{\rm IC}$ and $Q_{\rm IC}$, the beaming direction of the TeV photons is as follows:

$$\cos\theta_{\rm IC} = \frac{e^{\mu}_{(r)}P^{\rm IC}_{\mu}\Big|_{r_{\rm c}}}{-e^{\mu}_{(t)}P^{\rm IC}_{\mu}\Big|_{r_{\rm c}}} = \frac{\pm\mathcal{R}(r)^{1/2}}{A^{1/2}(1-\omega\lambda_{\rm IC})}, \tag{8}$$

$$\sin\theta_{\rm IC}\cos\phi_{\rm IC} = \frac{e^{\mu}_{(\theta)}P^{\rm IC}_{\mu}\Big|_{r_{\rm c}}}{-e^{\mu}_{(t)}P^{\rm IC}_{\mu}\Big|_{r_{\rm c}}} = \frac{\pm\Theta(\theta)^{1/2}\Delta^{1/2}}{A^{1/2}(1-\omega\lambda_{\rm IC})}, \tag{9}$$

$$\sin\theta_{\rm IC}\sin\phi_{\rm IC} = \frac{e^{\mu}_{(\phi)}P^{\rm IC}_{\mu}\Big|_{r_{\rm c}}}{-e^{\mu}_{(t)}P^{\rm IC}_{\mu}\Big|_{r_{\rm c}}} = \frac{\lambda_{\rm IC}}{\sin\theta_{\rm c}}\frac{\Sigma\Delta^{1/2}}{A(1-\omega\lambda_{\rm IC})}, \tag{10}$$

where the trajectory of the TeV photons determined by $\lambda_{\rm IC}$ and $Q_{\rm IC}$ can be found by tracing the observed TeV photons from the infinity ($r=\infty, \theta_{\rm obs}=30^{\circ}$) to the interacting location ($r=r_{\rm c}, \theta=\theta_{\rm c}$). As assumed above, the TeV source is located inside the jet, therefore, $\theta_{\rm c}=0$ and subsequently $\lambda_{\rm IC}=0$.

After determining the trajectory $(\lambda_{\rm IC}, Q_{\rm IC})$ of the TeV photons, the corresponding redshift factor $g_{\rm IC}$ for the γ-ray photons traveling from the IC interaction location to the infinity is given by

$$g_{\rm IC} = \frac{\nu^{\rm IC}_{\infty}}{\nu^{\rm IC}_{r_{\rm c}}} = \frac{e^{\mu}_{(t)}P^{\rm IC}_{\mu}\Big|_{\infty}}{e^{\mu}_{(t)}P^{\rm IC}_{\mu}\Big|_{r_{\rm c}}} = \frac{\Sigma^{1/2}\Delta^{1/2}}{A^{1/2}}\frac{1}{1-\omega\lambda_{\rm IC}}\Big|_{r_{\rm c}}. \tag{11}$$

3.4. *Spectrum of Compton-scattered external radiation fields*

Given the radiation energy of the soft photons and the energy distribution of the high energy electrons, the Compton spectral luminosity is given by (see Finke et al. 2008 and Dermer et al. 2009 for more details):

$$f^{\rm EC}_{local}(\epsilon_{\rm IC}) = \frac{\epsilon_{\rm IC}L_{\rm C}(\epsilon_{\rm IC},\Omega_{\rm IC})}{d_L^2} = \frac{c\pi r_e^2}{4\pi d_L^2}\,\epsilon^2_{\rm IC}\delta^3_{\rm D}\int_0^{2\pi}d\phi_s\int_{-1}^{1}d\mu_s\int_0^{\epsilon_{s,hi}}d\epsilon_s\,\frac{I_{\nu_{\rm d}}g_{\rm s}^3}{\epsilon_{\rm s}^2}\int_{\gamma_{\rm low}}^{\infty}d\gamma\,\frac{N'_e(\gamma')}{\gamma^2}\,\Xi\,, \tag{12}$$

where $\epsilon_{\rm s}$ is the energy of the soft photons, $\epsilon_{\rm IC}$ is the energy of the γ-ray photons created via the IC process, $\mu_{\rm s}=\cos(\theta_{\rm s})$, and $\mu_{\rm IC}=\cos(\theta_{\rm IC})$. With the approximation that scattered photons travel in the same direction as the VHE electrons, the Compton cross section can be drawn as (Dermer et al. 1993 ; Dermer et al. 2006)

$$\frac{d\sigma_{\rm IC}(\epsilon_{\rm s},\epsilon_{\rm IC},\gamma,\psi_{\rm IC})}{d\epsilon_{\rm IC}} \cong \frac{\pi r_e^2}{\gamma\bar{\epsilon}}\,\Xi\;,\;\left(\frac{\bar{\epsilon}}{2\gamma}<\epsilon_{\rm IC}<\frac{2\gamma\bar{\epsilon}}{1+2\bar{\epsilon}}\right) \tag{13}$$

$$\bar{\epsilon}\equiv\gamma\epsilon_{\rm s}(1-\sqrt{1-1/\gamma^2}\cos\psi_{IC})\cong\gamma\epsilon_{\rm s}(1-\cos\psi_{\rm IC}), \tag{14}$$

where

$$\Xi \equiv y+y^{-1}-\frac{2\epsilon_{IC}}{\gamma\bar{\epsilon}y}+\left(\frac{\epsilon_{IC}}{\gamma\bar{\epsilon}y}\right)^2, \tag{15}$$

$$y \equiv 1-\frac{\epsilon_{IC}}{\gamma}, \tag{16}$$

and $\psi_{\rm IC}$ is the interaction angle between the VHE electron and the soft photon during the IC process.

$$\cos\psi_{\rm IC}=\mu_{\rm IC}\mu_s+\sqrt{1-\mu_{IC}^2}\sqrt{1-\mu_s^2}\cos(\phi_{IC}-\phi_s)\,, \tag{17}$$

The optical depth $\tau(\epsilon_{\rm IC}, H_{\rm TeV}, a)$ of these γ-ray photons ($\epsilon_{\rm IC}$) can be integrated along their trajectories as in Li et al. (2009),

$$\tau_{\gamma\gamma}(\lambda_{\rm IC},Q_{\rm IC},\epsilon_{\rm IC}) = \iiint(1-\cos\psi_{\gamma\gamma})\sigma_{\gamma\gamma}(\epsilon_s,\epsilon_{\rm IC},\psi_{\gamma\gamma})\frac{I_{\nu_{\rm d}}}{c\epsilon_s}g_{\rm s}^3{\rm d}\Omega_{\rm s}{\rm d}\epsilon_{\rm s}{\rm d}l, \tag{18}$$

where ${\rm d}l=e^{\nu}\Sigma{\rm d}\mathscr{T}$ is the proper length differential with ${\rm d}\mathscr{T}$ defined to be differential of the affine parameter $\mathscr{T}$ along the trajectory of the TeV photons, and $\psi_{\gamma\gamma}$ is the interacting angle between the TeV photon ($\epsilon_{\rm IC}$) and the soft photon ($\epsilon_{\rm s}$).

Consequently, the final observed SED in the infinity would be,

$$f^{\rm EC}_{\rm Earth}\left(\epsilon_{\rm IC}\frac{g_{\rm IC}}{1+z}\right) = e^{-\tau(\epsilon_{\rm IC})}\left(\frac{g_{\rm IC}}{1+z}\right)^4 f^{\rm EC}_{local}(\epsilon_{\rm IC}). \tag{19}$$

4. NUMERICAL RESULTS

4.1. $H_{\rm TeV}, a$ *dependence*

In this paper, we choose the BH spin as $a=0,\ 0.8,\ 0.998$ to be consistent with the ADAF model used in fitting the SED (from radio to X-ray) of M87 in Li et al. (2009). The location of the TeV source is set to be very close to the BH as $H_{\rm TeV}=5, 10, 20, 50,$ and $100R_g$, respectively. The distribution of the VHE electrons is described by $N_0=0.4\times10^{50}$, $\gamma'_{\rm min}=10^4$, and $p=-3.2$, where the maximal index p is chosen to fit the very flat TeV flare spectrum observed in 2005 and 2008 (Giannios et al. 2010).

In Fig. 3, we show the dependence of the SED of the EIC scattering on the height of the TeV source and BH spins. We can find that the efficiency of the Compton-scattering increases dramatically if the TeV source is closer to the disk. Furthermore, if the location of the TeV source $H_{\rm TeV}$ is below $20R_{\rm g}$, the Compton-scattered luminosity of the soft radiation fields from the the disk

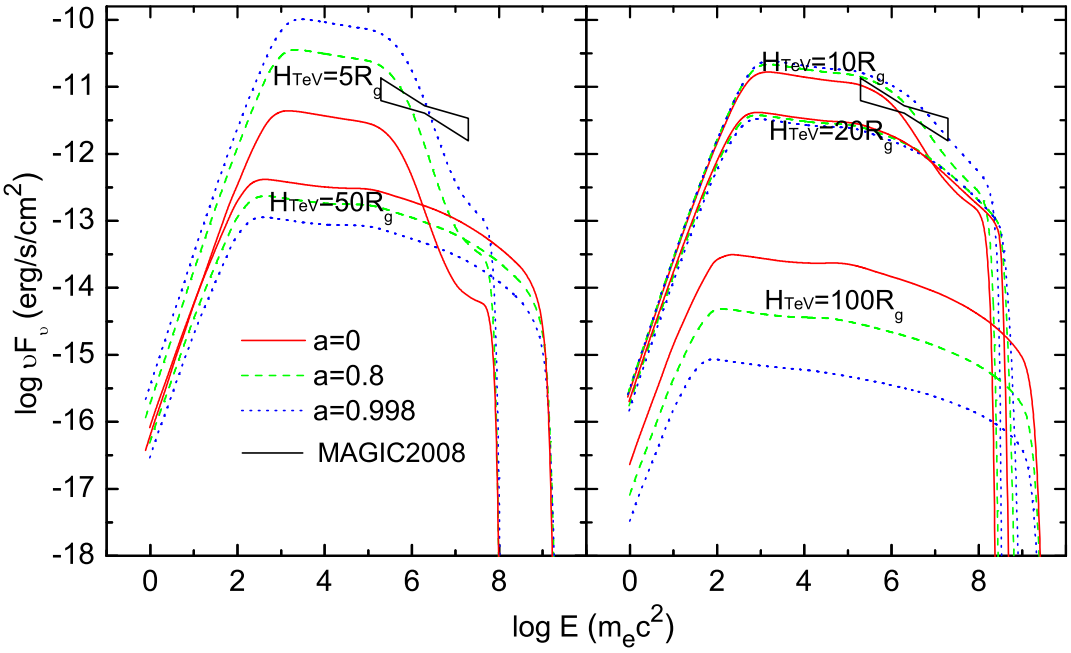

FIG. 3.— SED of the external Compton-scattering model with the different spins of the black hole ($a = 0, 0.8, 0.998$) and the location of the mini-jets is above the black hole (*Left panel:* $H_{\rm TeV} = 5, 50R_{\rm g}$, *right panel:* $H_{\rm TeV} = 10, 20, 100R_{\rm g}$). The energy distribution of the VHE electrons are determined by three parameters: $N_0 = 0.4 \times 10^{50}$, $\gamma_{\rm min} = 10^4$ and $p = -3.2$. The Lorentz factor of the mini-jets in the laboratory frame is taken to be $\Gamma_{\rm em} = 12$. MAGIC observation in 2008 is shown in the symbol of butterfly (Albert et al. 2008).

around the black hole with spin $a = 0.998$ is higher than that from the black hole with spin $a = 0$; meanwhile, if the location of the TeV source is higher than $20R_{\rm g}$, for $a = 0$, the Compton-scattered luminosity is higher than that for $a = 0.998$. This is because for $a = 0.998$, the soft radiation field from the disk is more compact, i.e., the soft radiation field is strong in the vicinity of the BH, however, at the distance far away from the disk, the region of the soft radiation field looks like a point source. Therefore, the colliding angle between the soft photons and the VHE electrons in the mini-jets is smaller, which reduces the rate of the inverse Compton scattering significantly.

It is also clearly shown in Fig. 3 that each spectrum has an exponential cut off beyond $E_{\rm cut} \sim 10^{8\sim9} m_{\rm e}c^2$ which is caused by the $\gamma\gamma$ absorption. If the location of the TeV source is nearer to the BH ($H_{\rm TeV} < 20R_{\rm g}$), the spectrum will also suffer from the severe $\gamma\gamma$ absorption in the observable band $0.1-10$TeV. In each of those reduced spectrums of $H_{\rm TeV} = 5, 10$, there is always a warp up trend at $E_{\rm IC} \sim 10^8 m_{\rm e}c^2$ which is caused by the relatively low optical depth $\tau_{\gamma\gamma}$ at that band, since the spectrum of the disk has a relatively low luminosity at $E_{\rm s} \sim 10^{-2} m_{\rm e}c^2$.

4.2. *TeV flares and The X-ray companion*

In 2008, observations had shown that the TeV, X-ray, and radio flares are well correlated (Acciari et al. 2009), though no X-ray correlation was found in 2005. We propose that the accompanying X-ray flare in 2008 results from the synchrotron radiation of the VHE electrons in the mini-jets, in other words, the X-ray flare could be a byproduct of the TeV flare, which just happens to be above the background X-ray flux. While in 2005, it is more likely the X-ray flaring flux is below the more stable X-ray background which is attributed to the disk and/or the corona. It is notified that the TeV flare in 2008 is stronger than that in 2005, and the corresponding X-ray flare is rather mild: during the flaring, the X-ray flux only increased about two times above the average.

In Fig. 4, both the SED of the direct synchrotron radiation and the Compton-scattered radiation are shown. We choose $H_{\rm TeV} = 20, 50$ to be as close to the BH as possible while avoid severe $\gamma\gamma$ absorption. Owing to the weak $\gamma\gamma$ absorption, all the EIC spectra have inherited the original power-law index of the VHE electrons, which is $p = -3.2, -3.5$. As expected, the corresponding synchrotron spectrum fitting the X-ray flares in 2008 is comparable with or exceeds the average X-ray flux, while the X-ray flux in 2005 is buried beneath the background flux.

The magnetic field in the mini-jets is taken to be $B = 1.6, 4, 2.6, 8$G, respectively, which is used to calculate the direct synchrotron radiation. The strength of the magnetic field used in this work is consistent with that in the original mini-jet model $B_{\rm em}$ (Giannios et al. 2010, and references therein), that is, $\lesssim 0.8(L_{\rm j,iso}/10^{45}\ {\rm erg/s})^{1/2}(100R_{\rm g}/r_{\rm jet})(5/\Gamma_j)^2$ G. We propose that the base of jet is cone shaped as $r_{\rm jet} \sim 0.5 H sin\theta_{\rm open}$, where the full opening angle $\theta_{\rm open} \sim 30^\circ$ (Acciari et al. 2009), which leads to $B(50R_{\rm g}) \lesssim 6.4$G, $B(20R_{\rm g}) \lesssim 16$G. The more detailed parameters are shown in Table 1.

There are four main parameters $N_0, p, H_{\rm TeV}, a$ in our models. Where the spin a is fixed because it only slightly influence the SED for $H_{\rm TeV} = 20, 50$ as shown in Fig. 3; the electron power-law index p is fixed to follow the observed TeV spectrum index

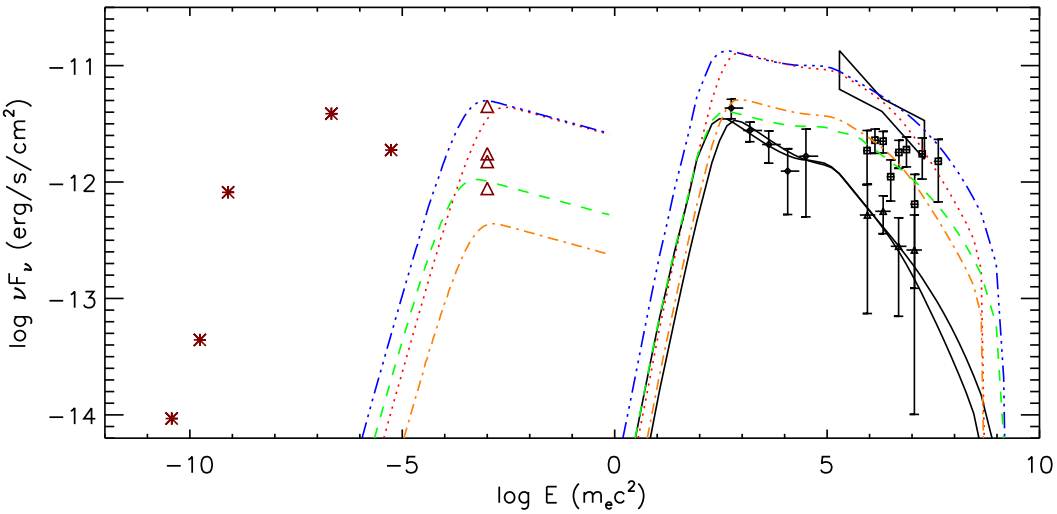

FIG. 4.— Synchrotron (dashed lines and dash-dotted lines) and the external Compton-scattered (solid lines and dotted lines) emission from a Mini-jet which are modeled to fit the observed emission from M87, the detailed model parameters are shown in Table one. The observed emission include: (1). MAGIC observation in 2008 which is shown in the symbol of butterfly (Albert et al. 2008); (2). HESS observation in 2005 which is indicated by the black square with long error-bars ; (3). HESS observation in 2004 which is labeled as the black triangle with long error-bar (Aharonian et al. 2006); (4). FERMI observation in 2009 which is labeled as the black solid circle with error-bars (Abdo et al.2009); (5). The approximate data from Chandra is shown in the hollow triangles. With 5% uncertainty, the one on the top represent the flux of nucleus in 2008 Feb 16 (data are provided by Dr. D. E. Harris), the other three represent the flux in 2005 Apr 22, Apr 28, May 04 separately (Harris et al. 2006, 2009); (6). Typical nucleus emission is shown in the asterisk.(Harms et al. 1994; Maoz et al. 2005; Reynolds et al. 1996; Sparks et al. 1996). The synchrotron-self Compton emission is too weak to be shown in this figure.

TABLE 1
MODEL PARAMETERS USED IN FITTING THE OBSERVATIONS SHOWN IN FIG.4.

EIC lines in Fig.4	$H_{\rm TeV}(R_{\rm g})$	$\gamma_{\rm min}$	N_0(counts)	p	$B(G)$
Fitting 2008MAGIC[a] with two lines on the top					
dash-3doted line	50	10^4	1.0×10^{51}	-3.2	2.6
dotted line	20	10^4	1.0×10^{50}	-3.2	8
Fitting 2005HESS[b] with two lines in the middle					
dashed line	50	10^4	0.6×10^{51}	-3.2	1.6
dash-dotted line	20	10^4	0.4×10^{50}	-3.2	4
Fitting 2004HESS[c]+2009FERMI[d] with two lines at the bottom					
solid line	50	10^4	1.6×10^{52}	-3.5	–
solid line	20	10^4	0.5×10^{51}	-3.5	–

NOTE. — The bulk speed of the mini-jets in local lab frame is taken as $\Gamma_{\rm mini}=12$ and the viewing angle is set as $\theta_{\rm obs}=30^\circ$. The parameter spin of the BH is chosen as $a=0.8$, because the changing of the spin barely influence the shape of the spectrum, it just slightly boost the entire SED up or down when applying $H_{\rm TeV}=20,50R_g$.

[a] MAGIC observation of M87 in 2008, as a flaring state
[b] HESS observation of M87 in 2005, as a flaring state
[c] HESS observation of M87 in 2004, as a quiet state
[d] FERMI observation of M87 in 2009, as a quiet state

and the $\gamma\gamma$ absorption is too low to soften the spectrum; the other two parameters N_0 and $H_{\rm TeV}$ are degenerated, making it hard to draw any solid constrains by fitting the SED. To be more specific, the final TeV flux should be roughly $F_{\rm IC}\sim N_0/H_{\rm TeV}^2$. As shown in Table 1, to fit the same observation data, when the $H_{\rm TeV}$ changes from $20R_{\rm g}$ to $50R_{\rm g}$, we need about 10 times more VHE electrons. Therefore, considering that both the TeV flares in 2005 and 2008 have the same a and $p(-2.2\sim-2.6)$, we suggest that the TeV source in 2008 may be more powerful or/and be closer to the BH.

Being closer to the BH, the TeV source will suffer more $\gamma\gamma$ absorption, which would soften the spectrum. But no obvious changes of the spectrum index can be drawn from the observations in 2005 and 2008 due to the long error-bars. It is noticed that, as shown in Fig. 3, the $\gamma\gamma$ absorption barely influences the γ-ray spectrum below 0.1 TeV, therefore the Fermi telescope should be able to provide better constrains on the power-law index of the VHE electrons.

As shown in Fig. 4, we also fit the quiet state (2004HESS+2009FERMI) spectrum of M87 with the mini-jets model. In other words, the quiet TeV flux could be attributed from some mini-jets which are weaker, misaligned, or heavily absorbed by synchrotron or/and $\gamma\gamma$ pair production (lower $N_{\rm e,p},\delta_D$). Where the misaligned Mini-jets could be considered as weaker mini-jets consisted of much fewer VHE electrons beaming towards us with lower bulk velocity, see details in (Giannios et al. 2010).

Therefor we could not exclude the possibility that weaker flares are due to misaligned mini-jets, which are supposed to have lower $\delta_{\rm D}$. It should be noticed that lower $\delta_{\rm D}$ could not explain the steeper spectrum.

As mentioned above, the soft photons field are demanded to satisfy both the low $\gamma\gamma$ absorption rate and the high IC cooling efficiency. In models as shown in Fig. 4, apparently, the synchrotron cooling effect is not dominating since the EIC flux is much higher. The IC cooling time is short enough so that there is no influence on the observed rapid variation ($1 \sim 2$days):

$$E_{\rm e} \sim L_{\rm GeV-TeV} t_{\rm cool}/(4\Gamma_{em}^2),\ \ E_{\rm e} \sim \Gamma_{\rm em} \int_{10^4}^{\infty} \gamma' N'_e(\gamma') d\gamma',\ \ t_{\rm cool} < t_{\rm var}, \tag{20}$$

where $L_{\rm GeV-TeV}$ is the isotropic total EIC flux and $E_{\rm e}$ is the total energy of VHE electrons in the lab frame. With the parameters listed in Table 1, as expected, one can find $t_{\rm cool} \sim 10^{2-3}$s. During this cooling time, the mini-jets can only travel less than $\sim 0.5R_g$, which is consistent with the above assumption that the location of the TeV source keeps unchanged during a flare event.

5. CONCLUSIONS AND DISCUSSIONS

In this paper, by taking into account the fully general relativity effects, we propose a disk-dominating external Compton-scattering model for explaining the flat TeV radiation from M87. The external Compton-scattering model suffers much less self-$\gamma\gamma$ absorption, comparing to the one-zone self-synchrotron Compton model, in which the soft photons and the VHE electrons are from the same blobs. The advantage of the EIC model in which the soft radiation is from the accretion disk is that the soft radiation source could be more compact and further away from the TeV source than ones in the SSC models, in which the $\gamma\gamma$ absorption can be reduced significantly. Besides, our EIC model is also supported by the observed mild IR-UV-X flux variations of the nucleus and the large viewing angle of the jet of M87 (the nuclei flux with viewing angle 30° is unlikely to be contaminated by the jet, neither to be blocked by the disk itself). It should be noticed that the VHE electrons and TeV photons may be influenced by some outflows with the anisotropic radiation at the soft band which are not beaming towards us, such as the jet itself. Unfortunately, the base of the jet of M87 appears to be quite chaotic, thus it is hard to draw any conclusions about the detailed structure of jet/outflows (Perlman et al. 2011). In our model, the TeV sources are the mini-jets which are easily able to beam towards us with high Doppler factor and give rise to the observed VHE radiation.

How to distinguish between SSC and EIC models by the future observations? The main difference between these two models is that the IR-UV variation and TeV flares are not necessarily correlated in the EIC models, but they are in the SSC models, especially the multi-zone SSC model. Therefore, we can distinguish between the SSC and EIC models by the simultaneous observations of the IR-UV emission during the TeV flare. Unfortunately, during the 2005 TeV flares, there is no accompanied HST observation of M87. With the better sensitivity of CTA (it is about $>$10 times better than those of the present Cerenkov telescopes), we will be able to detect the fainter flares and obtain the minimal variation time scale of the TeV flares, which increases the opportunity of finding the correlated variation between IR-UV and TeV emission.

In our models, with little $\gamma\gamma$ absorption, all the EIC spectra at the observational band have inherited the original power-law index of the VHE electrons. After fitting those spectra, we calculate the cooling time of the VHE electrons in the mini-jets (see section 4) to make sure that they would not travel longer than $ct_{\rm var}\delta_D$. It turns out when TeV source is located at $H_{\rm TeV} < 50R_{\rm g}$, the IC cooling time is very much shorter than the upper-limits of the observed TeV variation of 1-2 days. Therefore, if possibly, the TeV source is located further away from the disk ($H_{\rm TeV} > 50R_{\rm g}$), the cooling efficiency of the VHE electrons in the mini-jets is much lower, the mini-jets could move out of the main jet. As a result, the variation of the soft radiation background at the different locations above the disk should be considered.

We also discuss the probability that the direct synchrotron radiation from the mini-jets may cause the correlated X-ray flare in 2008. As expected, according to our model, if the magnetic field is about several Gauss, the direct synchrotron flux from these mini-jets which lies at the X-ray band can explain the X-ray flare very well but has no influence on the observed radiation at the GeV-TeV band. However, the magnetic field B can not be constrained by any direct observation, as discussed above, and we only have a rough estimate of the strength of the magnetic field supposed to be consistent with the mini-jets model. Considering that the synchrotron flux is roughly about $F_{\rm syn} \sim N_0 B^2$, it is obvious that the N_0 and B are degenerated. If the TeV source is confined inside the region $20R_g < H_{\rm TeV} < 50R_{\rm g}$, the corresponding strength of the magnetic field is required to be about $2G < B < 8G$, in order to produce the X-ray flare in 2008.

Dealing with the two weeks data of the 2008 flare from MAGIC, Albert et al. (2008) had separated the high state data ($\sim$ 1 day time scale) from the low state data and they found that during the high states, the spectra are harder: the spectrum index of the high state is about 2.2, while that of the low state is about 2.6. Because the IC cooling time and the synchrotron cooling time of VHE particles is short, the observed fastest variation should be dominated by the time of the acceleration, or even the shifting of the beaming angle of the mini-jets. If there is no continuous acceleration of the relativistic electrons, the spectra of the TeV flares will become steeper. In the year of 2008, VERITAS captured the TeV flare (Feb 9-13, 2008) which is close to the date of the X-ray flare (Feb 16, 2008). VERITAS observation shows that the spectrum index of the TeV flare is about 2.4, which is softer than the earlier flares captured by MAGIC (Acciari et al. 2010). We suggest that the TeV flare captured by VERITAS is happening during the rapid synchrotron cooling of the relativistic electrons in the mini-jet, and the X-ray flare could be a byproduct of that TeV flare, as the X-ray flares in 2008. Our suggestion could naturally explain the X-ray excess and the softer spectrum of TeV emission. There are two ways to check above suggestion: first, the flux of the X-ray via synchrotron radiation should be anti-correlated with the TeV flux via EIC, which could be tested by the future observations with the higher time resolution (less than 1 day); second, and the TeV flare should share the similar spectrum index with that of the X-ray flare. Unfortunately, due to the pile up effect of X-ray observation (Harris et al. 2009), we can not obtain the correct spectrum index of the X-ray flare.

We would like to thank the anonymous referee for her/his constructive suggestions and comments, and Dr. Daniel Harris for providing his preliminary results on *Chandra* observations of M87. This work is partially supported by National Basic Research Program of China (2009CB824800), the National Natural Science Foundation (11073020,10733010,11133005), and the Fundamental Research Funds for the Central Universities (WK2030220004).

REFERENCES

Abdo, A. A., et al. 2009, ApJ, 707, 55
Abramowski, A., Acero, F., Aharonian, F. et al. 2011, arXiv:1111.5341
Acciari, V. A., et al. 2009, Science, 325, 44
Acciari, V. A., Aliu, E., Arlen, T., et al. 2010, ApJ, 716, 819
Aharonian, A. et al. 2006, Science, 314, 1424
Aharonian, F., et al. 2007, ApJ, 664, L71
Aharonian, F., et al. 2009, ApJ, 695, L40
Albert, J., et al. 2008, ApJ, 685, L23
Aleksić, J., Antonelli, L. A., Antoranz, P., et al. 2010, ApJ, 723, L207
Aliu, E., Anderhub, H., Antonelli, L. A., et al. 2009, ApJ, 692, L29
Bardeen, J. M., Press, W. H., & Teukolsky, S. A. 1972, ApJ, 178, 347
Barkov, M. V., Aharonian, F. A., & Bosch-Ramon, V. 2010, ApJ, 724, 1517
Bicknell, G. V. & Begelman, M. C. 1996, ApJ, 467, 597
Begelman, M. C., Fabian, A. C., & Rees, M. J. 2008, MNRAS, 384, L19
Beilicke, M., et al. 2010, Bulletin of the American Astronomical Society, 42, 702
Bromberg, O., & Levinson, A. 2009, ApJ, 699, 1274
Cheung, C. C., Harris, D. E., & Stawarz, Ł. 2007, ApJ, 663, L65
Dermer, C. D., et al. 2009, ApJ, 692, 32
Dermer, C. D., Böttcher, M. 2006, ApJ, 643, 1081
Dermer, C. D., & Schlickeiser, R. 1993, ApJ, 416, 458
Di Matteo, T., Allen, S. W., Fabian, A. C., Wilson, A. S., & Young, A. J. 2003, ApJ, 582, 133
Finke, J. D., Dermer, C. D., Böttcher, M. 2008, ApJ, 686, 181
Fossati, G., et al. 2008, ApJ, 677, 906
Gebhardt, K., & Thomas, J. 2009, ApJ, 700, 1690
Georganopoulos, M., Perlman, E. S., & Kazanas, D. 2005, ApJ, 634, L33
Giannios, D., Uzdensky, D. A., & Begelman, M. C. 2009, MNRAS, 395, L29
Giannios, D., Uzdensky, D. A., & Begelman, M. C. 2010, MNRAS, 402, 1649
Harris, D. E., Cheung, C. C., Stawarz, Ł., Biretta, J. A., & Perlman, E. S. 2009, ApJ, 699, 305
Harris, D. E., Cheung, C. C., Biretta, J. A., Sparks, W. B., Junor, W., Perlman, E. S., & Wilson, A. S. 2006, ApJ, 640, 211
Harris, D. E., F. Massaro, C. C. Cheung, et al. 2011, arXiv1111.5343H
Harms, R. J. et al. 1994, ApJ, 435, L35
Hinton, J. A., & Hofmann, W. 2009, ARA&A, 47, 523
Junor, W., Biretta, J. A., & Livio, M. 1999, Nature, 401, 891
Katarzyński, K., Sol, H., & Kus, A. 2001, A&A, 367, 809
Lenain, J.-P. 2007, SF2A-2007: Proceedings of the Annual meeting of the French Society of Astronomy and Astrophysics , 196
Li, Y.-R., Yuan, Y.-F., Wang, J.-M., Wang, J.-C., & Zhang, S. 2009, ApJ, 699, 513
Ly, C., Walker, R. C., & Junor, W. 2007, ApJ, 660, 200
Macchetto, F., Marconi, A., Axon, D. J., Capetti, A., Sparks, W., & Crane, P. 1997, ApJ, 489, 579
Maoz, D., Nagar, N. M., Falcke, H. & Wilson, A. S. 2005, ApJ, 625, 699
Neronov, A. & Aharonian, F. A. 2007, ApJ, 671, 85
Owen, F. N., Eilek, J. A., & Kassim, N. E. 2000, ApJ, 543, 611
Perlman, E. S., Adams, S. C., Cara, M., et al. 2011, arXiv:1109.6252
Reimer, A., Protheroe, R. J., & Donea, A.-C. 2004, A&A, 419, 89
Reynolds, C. S., Fabian, A. C., Celotti, A. & Rees, M. J. 1996, MNRAS, 283, 873
Rieger, F. M. & Aharonian, F. A. 2008, A&A, 479, L5
Sparks, W. B., Biretta, J. A. & Macchetto, F. 1996, ApJ, 473, 254
Stawarz, Ł., Aharonian, F., Kataoka, J., et al. 2006, MNRAS, 370, 981
Tsvetanov, Z. I., Hartig, G. F., Ford, H. C., Dopita, M. A., Kriss, G. A., Pei, Y. C., Dressel, L. L., & Harms, R. J. 1998, ApJ, 493, L83
Tavecchio, F., Maraschi, L., & Ghisellini, G. 1998, ApJ, 509, 608
Tavecchio, F., & Ghisellini, G. 2008, MNRAS, 385, L98
Wang, J.-M., Li, Y.-R., Wang, J.-C., & Zhang, S. 2008, ApJ, 676, L109
Yuan, Y.-F., Cao, X., Huang, L., & Shen, Z.-Q. 2009, ApJ, 699, 722